

Small-molecule probes for apoptosis:

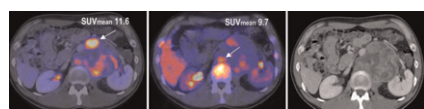
Reshef and colleagues provide an overview of current approaches in developing highly specific probes suitable for clinical PET imaging of apoptosis and emphasize the importance of multidisciplinary contributions. **Page 837**

Monitoring response with ^{18}F -FLT PET:

Weber reviews current work and highlights unanswered questions about the utility of this tracer for imaging tumor cell proliferation in a range of research and clinical oncologic applications. . **Page 841**

^{18}F -FLT PET/CT in germ cell tumors:

Pfannenberger and colleagues determine the value added by imaging with this tracer to ^{18}F -FDG PET in early response monitoring and prediction in patients with metastatic germ cell tumors. **Page 845**

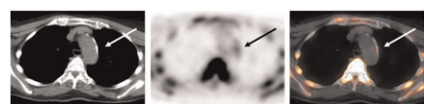


Nonlaxative PET/CT colonography:

Taylor and colleagues investigate the technical feasibility and diagnostic performance of combined nonlaxative PET/CT colonography in patients at higher risk of colorectal neoplasia. **Page 854**

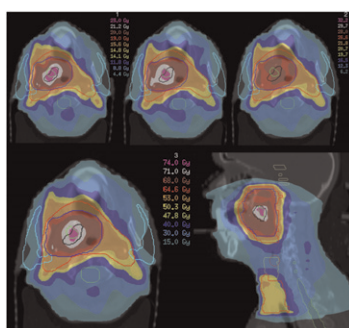
PET/CT plaque imaging:

Derlin and colleagues assess ^{18}F -sodium fluoride PET/CT for imaging mineral deposition in arterial wall alterations and the potential of this technique to provide relevant information about morphologic and functional properties of calcified plaque. **Page 862**



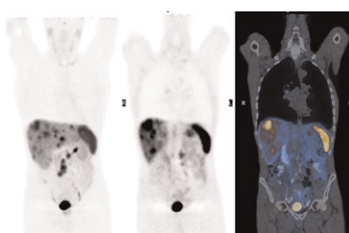
^{18}F -FLT PET/CT in oropharyngeal cancer:

Troost and colleagues monitor early response with serial ^{18}F -FLT PET/CT imaging in patients with oropharyngeal tumors to identify subvolumes with high proliferative activity eligible for dose escalation. **Page 866**



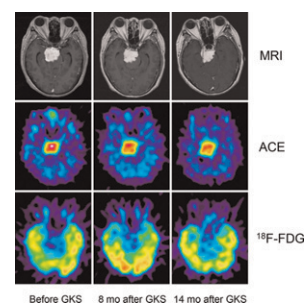
^{68}Ga -DOTATATE PET in NETs:

Srirajskanthan and colleagues evaluate the role of ^{68}Ga -DOTATATE PET in patients with negative or weakly positive findings on ^{111}In -DTPA-octreotide scintigraphy to determine whether PET detects additional disease and positively affects management decisions. **Page 875**



^{11}C -acetate PET and meningiomas:

Liu and colleagues compare the merits of this PET tracer and those of ^{18}F -FDG in detection of meningiomas and in monitoring the effects of γ -knife radiosurgery. **Page 883**



Clinical imaging of *HER2* expression:

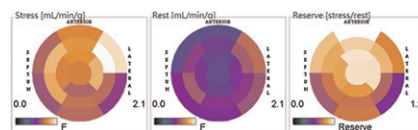
Baum and colleagues investigate the utility of a human epidermal growth factor receptor 2–targeting Affibody molecule for detection and characterization of *HER2*-positive lesions in patients with recurrent metastatic breast cancer. **Page 892**

^{82}Rb PET/CT reference ranges:

Bravo and colleagues establish reference values for left ventricular ejection fraction, end-systolic volume, and end-diastolic volume using 4 different commercial software packages and assess 2 approaches for defining a “healthy” individual. **Page 898**

PET and cardiac allograft vasculopathy:

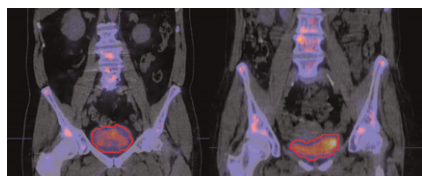
Wu and colleagues evaluate the efficacy of dynamic ^{13}N -ammonia PET in identifying early stages of allograft vasculopathy and discuss the potential for beneficial management decisions after heart transplantation. **Page 906**



^{18}F -AV-45 AD imaging:

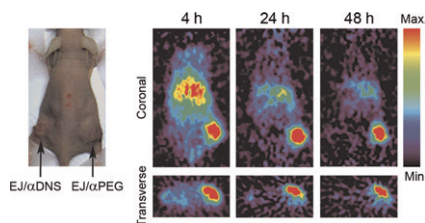
Wong and colleagues describe the results of a study of this amyloid- β PET tracer in cognitively healthy controls and patients with Alzheimer disease to determine its ability to provide objective measures for evaluation of late-life cognitive impairment. **Page 913**

Quantitative accuracy of ^{99m}Tc SPECT/CT: Zeintl and colleagues present a calibration method for quantitative ^{99m}Tc SPECT in a clinical SPECT/CT device, including ordered-subset expectation maximization with depth-dependent 3D resolution recovery, CT-based attenuation correction, and scatter correction. **Page 921**



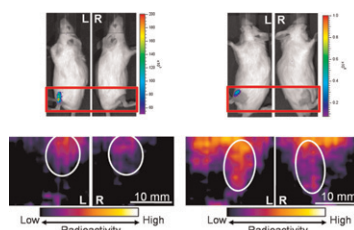
Variations in dosimetry with obesity: Clark and colleagues describe dose assessment phantoms that model the influence of obesity on specific absorbed fractions and dose factors in adults. **Page 929**

Anti-polyethylene glycol reporter gene: Chuang and colleagues describe the construction of a versatile and nonimmunogenic reporter gene to noninvasively image gene expression or cell delivery by optical imaging, MR imaging, and small-animal PET. **Page 933**



HER1-targeted immunoPET: Nayak and colleagues report on preclinical development of ^{86}Y -CHX-A''-DTPA-panitumumab for quantitative PET of epidermal growth factor receptor-expressing carcinoma. **Page 942**

Novel gene delivery and PET: Watanabe and colleagues outline a new methodology for gene therapy, using nanobubbles and ultrasound for nonviral gene delivery and PET and bioluminescence imaging for gene transfer detection. **Page 951**

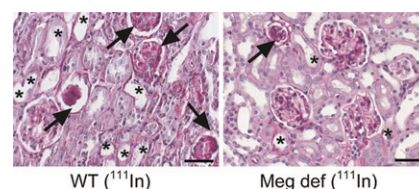


Imaging VEGFR after sunitinib: Levashova and colleagues determine whether noninvasive SPECT of vascular endothelial growth factor receptors, a target of anti-angiogenic drugs, can provide real-time information on tumor responses to treatment. **Page 959**

ImmunoPET with ^{124}I -ch806: Lee and colleagues describe a PET-based method for detecting a constitutively active epidermal growth factor receptor associated with disease progression and resistance to chemo- and radiotherapy in glioma. **Page 967**



Nephrotoxicity after ^{111}In SPECT: Melis and colleagues explore renal toxicity and radiation dose in a series of ^{111}In -labeled peptides using serial SPECT assessments in mice and discuss the implications for long-term renal damage with this tracer. **Page 973**



Visualizing siRNA delivery: Kang and colleagues detail a novel ^{99m}Tc -radiolabeled method to image small-interference RNA targeting of a tumor biomarker of human telomerase reverse transcriptase in HepG2 tumor xenografts. **Page 978**

RIT survey: Schaefer and colleagues report the results of an e-mail survey assessing the opinions of U.S. oncologists and hematologists on experiences with and challenges to CD20-directed radioimmunotherapy. **Page 987**

ON THE COVER

Molecular imaging using the ^{111}In - or ^{68}Ga -labeled Affibody molecule ABY-002 has the potential to localize metastatic lesions in vivo, adds qualitative information not available by conventional techniques, and may allow the *HER2* status to be determined for metastases not amenable to biopsy. In the patient shown here, a potential metastasis in the chest wall near the axilla was shown with ^{68}Ga -ABY-002 but was not visible with ^{18}F -FDG.

See page 895.

